Influence of flow rate on different properties of diamond-like nanocomposite thin films grown by PECVD

T. S. Santra,[1] T. K. Bhattacharyya,[2] F. G. Tseng,[1,3] and T. K. Barik[4,a]
[1]*Institute of Nanoengineering and Microsystems (NEMS), National TsingHua University, Hsinchu, Taiwan*
[2]*Department of Electronics and Electrical Communication Engineering, Indian Institute of Technology, Kharagpur-721302, West Bengal, India*
[3]*Department of Engineering and Systems Science, National Tsing Hua University, Hsinchu, Taiwan*
[4]*School of Applied Sciences and Humanities, Haldia Institute of Technology, Haldia-721657, Purba Medinipur, West Bengal, India*

(Received 20 May 2011; accepted 1 May 2012; published online 17 May 2012)

Diamond-like nanocomposite (DLN) thin films were deposited on pyrex glass substrate using different flow rate of haxamethyldisiloxane (HMDSO) based liquid precursor with nitrogen gas as a glow discharged decomposition by plasma enhanced chemical vapor deposition (PECVD) technique. The significant influence of different precursor flow rates on refractive index and thickness of the DLN films was measured by using spectroscopic filmatrics and DEKTAK profilometer. Optical transparency of the DLN thin films was analyzed by UV-VIS-NIR spectrometer. FTIR spectroscopy, provides the information about shifted bonds like SiC_2, Si-C, Si-O, C-C, Si-H, C-H, N-H, and O-H with different precursor flow rate. We have estimated the hardness of the DLN films from Raman spectroscopy using Gaussian deconvolution method and tried to investigate the correlation between hardness, refractive index and thickness of the films with different precursor flow rates. The composition and surface morphology of the DLN films were investigated by X-ray photo electron spectroscopy (XPS) and atomic force microscopy (AFM) respectively. We have analyzed the hardness by intensity ratio (I_D/I_G) of D and G peaks and correlates with hardness measurement by nanoindentation test where hardness increases from 27.8 μl/min to 80.6μl/min and then decreases with increase of flow rate from 80.6μl/min to 149.5μl/min. Finally, we correlates different parameters of structural, optical and tribological properties like film-thickness, refractive index, light transmission, hardness, surface roughness, modulus of elasticity, contact angle etc. with different precursor flow rates of DLN films. [http://dx.doi.org/10.1063/1.4721654]

I. INTRODUCTION

Diamond-like carbon (DLC) is a metastable form of amorphous carbon or hydrogenated amorphous carbon, containing significant fraction of sp^3 bonds.[1] DLC films have been utilized industrially as a wear resistant coating for hard-disk drive, optical component and also in the form of biocompatible coatings for medical purpose because of their excellent properties like high hardness, low coefficient of friction (COF), high wear resistance, chemical inertness, good optical transparency etc.[2–7] But DLC films can't retain their all characteristics at higher temperature because of conversion of sp^3 hybridized carbon to sp^2 hybridized carbon. Although, DLC films have high intrinsic

[a]Corresponding author: Email: tarun.barik2003@gmail.com, santra.tuhin@gmail.com; ph. no.: +91-3224-252900 extn. 315/316; Fax no.: +91-3224-252800/253062

compressive stress between the films and substrate, which generally provide the poor adhesion between film and substrate.

Now a days, researchers are giving much more attention to develop new kind of thin films like diamond-like nanocomposite (DLN) compared to DLC thin films. DLN film consists of diamond-like carbon bonds chemically stabilized by hydrogen atoms and quartz-like silicon bonds chemically stabilized by oxygen atoms in a pure amorphous structure.[8–10] This films can be deposited by different techniques like plasma enhanced chemical vapor deposition,[9–12] plasma assisted chemical vapor deposition,[13,14] thermally activated chemical vapor deposition[15] etc. To achieve better film properties, researchers need to investigate the details parameters like precursor flow rate, chamber pressure, substrate temperature, which are very important for good quality microstructure of the films. The precursor flow rate of any chemical vapor deposition can affect the mechanical, structural and tribological properties of the films.[16,17] Hence, this study can help to understand the appropriate films properties at different flow rate conditions. The nitrogen, hydrogen and oxygen content into the films can be varied with different flow rates, which can dramatically change the films properties.

In this article, we have mainly investigated the shifts of different band by FTIR and Raman analysis. X-Ray photoelectron spectroscopy provides different composition of the thin films and we correlate this composition with film-thickness, refractive index, hardness, modulus of elasticity, surface roughness, contact angles, light transmission capabilities etc. at different flow rate conditions. The DLN film preparation and the details about the characterization techniques have been discussed in section II. Section III focuses on the experimental results about the optical, structural and tribological properties of the films. Finally, in section IV, we have briefly recapitulated our observations.

II. EXPERIMENTAL DETAILS

A. DLN film preparation

DLN films were deposited into pyrex glass substrate using hexamethayldisiloxane (HMDSO) based liquid precursor with nitrogen gas as a decomposition in glow discharge by plasma enhanced chemical vapor deposition (PECVD) technique. The molecular formula of HMDSO gas precursor is $(CH_3)_3$-Si-O-Si-$(CH_3)_3$.[10,18] This precursor is a organosilicon compound prepared by the hydrolysis of trimethylsilyl chloride. Initially, we have used standard cleaning process to clean the substrates (pyrex glass slides). At first the substrate was immerse in acetone for two minutes and then immerse in iso-propyl alcohol (IPA) for another two minutes. After that the substrate were rinsed in de-ionized (DI) water for three minutes and dried it by nitrogen blow. Next it was heated by hot plate at 120 °C for 5 minutes. The samples were further cleaned *in-situ* by argon plasma cleaning prior to DLN film deposition. For deposition of the films, we have used DC bias as well as RF bias voltage. For this DLN film deposition, we have used negative substrate bias of 650 volt for all samples by controlling the RF bias voltage. Substrate temperature was maintained at 250 °C by flowing cold water through the substrate holder assembly. The arrangement provides a planetary motion to the substrate holder plate in order to ensure uniform thickness of the film. Some important deposition parameters are given below.

i. Chamber pressure during growth: 4×10^{-4} Torr.
ii. Deposition time: 1 hour for each sample.
iii. RF power: 2×10^{3} Wm^{-2}.
iv. Precursor flow rates: varied from 27.8μl/min to 149.5 μl/min.

B. DLN film characterization

DLN film thickness and refractive index were measured by Filmatries and DEKTOK-3 profilometer, respectively. The transmission capability of the film was measured by UV-VIS-NIR spectroscopy (Jasco, V-670 spectrometer) with 400-2000 nm wavelength range. Contact angle of the DLN films was measured by dynamic contact angle analyzer (Edmund Scientific Co. N.J., USA). The structural change of the DLN films was determined by Fourier transform infrared spectroscopy

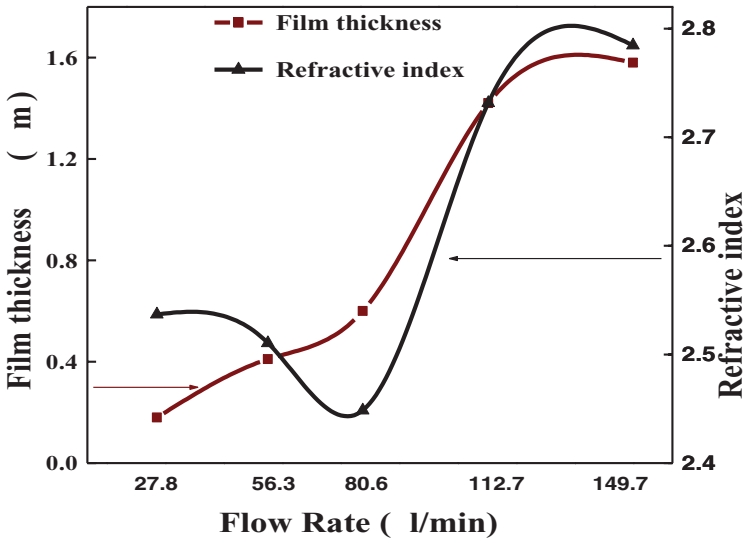

FIG. 1. Film thickness and refractive index variation with precursor flow rates of the DLN films deposited by PECVD technique.

(FTIR, Nexus 870) within 500-4000 cm^{-1} region. The Raman spectroscopy (Renishaw, LRM-1000B) with an argon ion laser source (50 mW power and green wavelength of 514.5 nm) was used to evaluate the material properties of the deposited DLN film within the wavenumber range 400-2000 cm^{-1}. The Raman parameters like peak position, FWHM and intensity ratio (I_D/ I_G) of D and G peaks (here D stands for disorder graphite band and G stand for asymmetrical single crystal graphitic band) of the DLN films, were estimated from the peak analysis using Gaussian line-shape deconvolution of Raman spectra.[19] The X-ray photoelectron spectroscopy (XPS) was carried out using ESCALAB MKII spectrometer,VG Scientific Ltd, U.K.). FTIR, Raman spectroscopy, XPS results conform to a large extent with structural model.[20,21] The surface morphology of the DLN films was investigated by atomic force microscopy (Agilent 5500, LS Picoplus) with tapping mode operation. Hardness of the deposited film was measured by nanoindentation XP (MTS System Corporation). The indentation tests were performed using berkorich-type diamond tip under an applied load of 20 mN with 300 nm depth into the film surface.

III. EXPERIMENTAL RESULTS AND DISCUSSIONS

A. Optical properties

Dimond-like nanocomposite (DLN) thin films, comprises the networks of hydrogenated amorphous carbon (a-C:H) and oxygenated amorphous silicon (a-Si:O), which we already proof in our previous articles.[9,10] In this article, we have mainly concentrated on material properties at different flow rates. In our experiment, we have studied a group of samples with different flow rates of hexamethayldisiloxane (HMDSO) based liquid precursor deposited by PECVD technique. From these samples, we have studied in details of five samples with different flow rates with their different properties. The flow rates dependent refractive index and thickness are given below in Fig. 1. From this figure, the thickness of the films slowly increases with the flow rates from 27.8 μl/min to 80.6 μl/min. After that thickness increases very sharply from 80.6 μl/min to 112.7 μl/min and then thickness is almost constant value with increase of the flow rates from112.7 μl/min to 149.5 μl/min. In the beginning the refractive index decreases with increase of the flow rates from 27.8 μl/min to 80.6 μl/min and then increases continuously with increase of the flow rate from 80.6 μl/min to 112.7 μl/min. After that flow rates decreases slowly from 112.7 μl/min to 149.5 μl/min. From Fig. 1 we have observed that the refractive index increases sharply with increase of thickness from 80.6 μl/min to 112.7 μl/min flow rate and both the parameters decreases slowly from 112.7 μl/min to 149.5 μl/min.

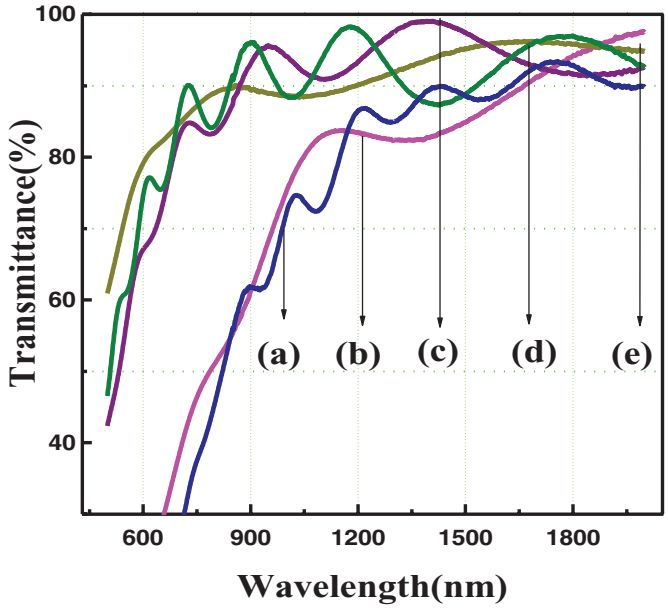

FIG. 2. UV-VIS-NIR spectra for light transmission through the DLN films with different flow rates (μl/min) (a) 27.8 (b) 56.3 (c) 80.6 (d) 112.7 (e) 149.5.

TABLE I. Optical transmission of DLN films at different precursor flow rates using UV-VIS-NIR spectroscopy.

Precursor flow rate (μl/min)	Light transmission (%)	Wavelength range (nm)	Average transmission (%)
27.8	80 - 90 %	1100 – 2000 nm	86
56.3	80 - 96 %	1020 – 2000 nm	90
80.6	80 - 92 %	680 – 2000 nm	94
112.7	80 - 93 %	667 – 2000 nm	93
149.5	80 - 93 %	590 – 2000 nm	93

Fig. 2 demonstrated the light transmission capability of the DLN films with different flow rates and we summarized the average light transmission capability (we took transmission values at different position of the wavelength range and average it for every samples) with different flow rates in Table I. At the beginning, the light transmission capability was 86% with 27.8 μl/min flow rate and the wavelength range was 1100-2000 nm for optical transmission. After increase of flow rates from 27.8 μl/min to 80.6 μl/min, the light transmission capability increases to 94% with increase of wavelength range (680-2000 nm). Then light transmission slightly decreases (93%) from flow rate 80.6 μl/min to 112.7 μl/min and finally the transmission remains constant (93%) upto 149.5 μl/min. But wavelength rage increases continuously (e.g. 590-2000 nm, at 149.5 μl/min). At higher flow rate, the transmission capability is higher (at 80.6 μl/min, 94%) compared to lower flow rate (at 27.8 μl/min, 86%), because it might be due to more oxygen and silicon content with less nitrogen content into the DLN films (see composition analysis by XPS). Finally, at flow rate 149.5 μl/min, the optical transparency becomes 93% with larger wavelength range about 590-2000 nm, because of less carbon content into the films.[22]

B. Structural properties

The structural characteristics were observed by the analysis of FTIR spectroscopy. This technique is a well known phenomenon for investigating the bond structure of atoms by using the IR absorption spectrum which is related to vibration of atoms.[23] FTIR spectra of DLN films with different precursors flow rates are shown in Fig. 3. From this structural analysis we have observed

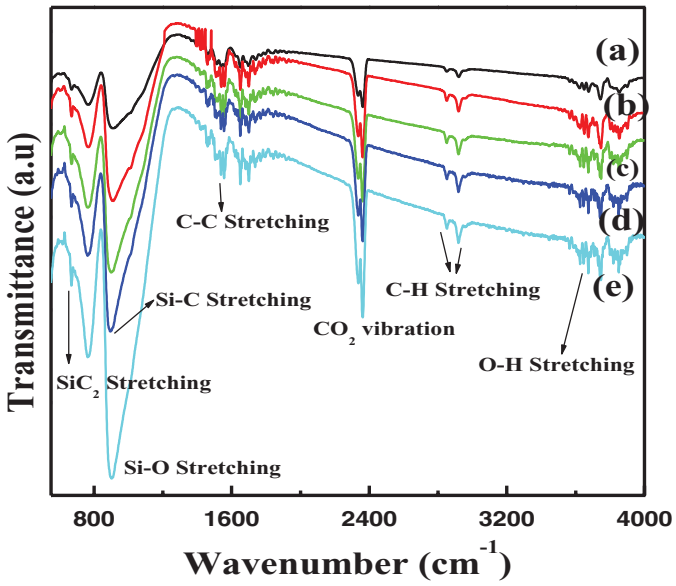

FIG. 3. FTIR spectra of the DLN films with different flow rates (μl/min) (a) 27.8 (b) 56.3 (c) 80.6 (d) 112.7 (e) 149.5.

TABLE II. Vibrational frequencies of the DLN films with different precursor flow rates using FTIR spectroscopy.

Flow Rate (μl/min)	SiC_2 (cm^{-1})	Si-C (cm^{-1})	Si-O (cm^{-1})	C-C (cm^{-1})	Si-H (cm^{-1})	C-H (cm^{-1})	N-H (cm^{-1})	O-H (cm^{-1})
27.8	620	766	910	1557, 1698	2202*	2852, 2921	3628	3748
56.3	616	763	885	1473, 1660	2178*	2852, 2911	3630	3724
80.6	598	756	879	1471, 1613	2102*	2850, 2916	3627	3703
112.7	604	764	899	1532, 1698	2160*	2850, 2919	3628	3747
149.5	608	768	906	1539, 1700	2165*	2850, 2920	3629	3743

*Very weak peak

that the DLN films mainly consists of SiC_2, Si-C, Si-H, Si-O, C-C, C-H, N-H and O-H stretching bonds. In Fig. 3, a narrow symmetric peak of SiC_2 appears at the wavenumber range of 608-620 cm^{-1} with different flow rates condition. The asymmetric Si-C stretching and rocking of CH_3 group appears at 766-768 cm^{-1} is due to Si-$(CH_3)_3$ vibrations.[9,10] The Si-O (Si-O-H) stretching appears at the range of 906-910 cm^{-1} with different flow rates and a very weak C=C stretching peak appears at 1560 cm^{-1}, which indicates non graphite bonding of carbon.[24] We have observed very week Si-H absorbance band which appears at the range of 2160-2202 cm^{-1} region. The Si-H stretching suggests that silicon is surrounded by some organic environment rather that incorporated in a silicon oxide network.[25,26] The CO_2 vibration occurs at the 2280-2400 cm^{-1} region due to atmospheric presence of carbon during the experiment. The C-H stretching bands appear at the rage of 2850-2919 cm^{-1}, which is very importance for DLN structural characterization. These types of vibrations included C-H_2 (symmetric), C-H_3 (symmetric), C-H_2 (asymmetric) and C-H_3 (asymmetric) stretching bands respectively. The N-H and O-H vibrations of the DLN films with different flow rates appears at the range of 3627-3629 cm^{-2} and 3703-3748 cm^{-2} regions, respectively. This type of vibration appears due to H and O content into the DLN films. The existence of N-H bond in the DLN films due to use of nitrogen decomposition in the glow discharge during film deposition.[27] Table II describes the details about peak vibrations of different bonding structures. However, this peak shifting needs more experimental verification in future for structural confirmation which are presenting now in our current article. Because of FTIR spectroscopy can give slightly peak shifting during different time to time experiment with same sample. Here we demonstrate the peak shifting with larger order of magnitude which we got during our experiment. In this table, the stretching bond of SiC_2, Si-C, Si-O,

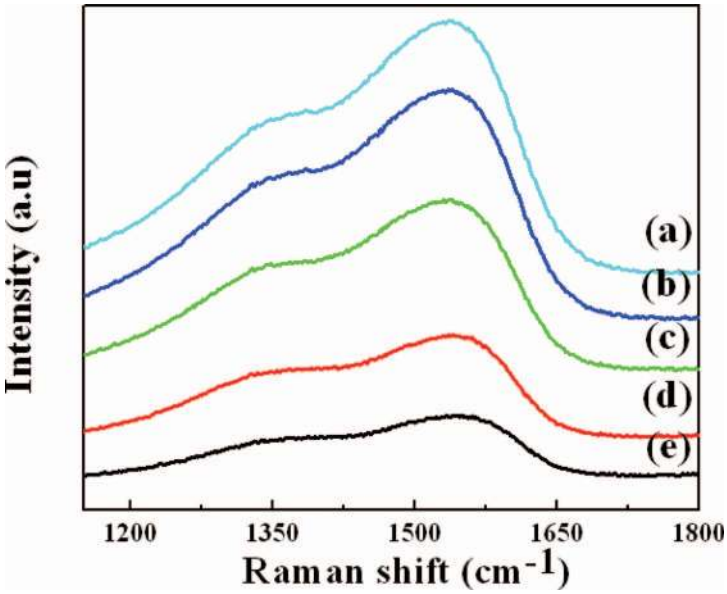

FIG. 4. Raman spectra of DLN films with different flow rates (μl/min) (a) 27.8 (b) 56.3 (c) 80.6 (d) 112.7 (e) 149.5.

C-C, Si-H and O-H stretching continuously decreases with flow rate from 27.8 μl/min to 80.6 μl/min and after that the wavenumber increases with continuous increase the flow rates from 80.6 μl/min to 149.5 μl/min. However the wavenumber for N-H stretching is almost same with increase of the flow rate. For C-H stretching, we found two very broad peaks mainly at and 2911-2921 cm^{-1} region. Where the wavenumber shift for first peak (2850-2852 cm^{-2}) are almost same for every samples but for second peak, the wavenumber decreases with increase flow rate from 27.8 μl/min to 56.3 μl/min and then the wavenumber increases with increase the flow rate from 56.3 μl/min to 149.5 μl/min. This bond shifts due to change of film composition with different flow rates (see XPS analysis). In this structural analysis, we have confirmed that, bond stretching wavenumber is minimum for every samples at flow rate 80.6 μl/min, which indicates the better film quality such as better hardness, surface roughness and modulus of elasticity(explain later in table-V). The C-H and Si-H bonds have confirmed that the films contains a-C:H and a-Si:O networks within the DLN films structure. The low compressive stress of the DLN films may be due to the incorporation of the nanoparticles into a-C:H and a-Si:O networks.[9,10,28]

The first order Raman spectra of DLN films with different flow rates are shown in Fig. 4. The spectra mainly consist of two broad bands around 1365-1400 cm^{-1} and 1534-1557 cm^{-1} with different precursor flow rates. These spectra are usually characterized by disorder graphite band (D band) and asymmetrical single crystal graphitic band (G band). From this Raman spectroscopy, we can analyze the state of carbon, because its sensitivity to the changes in translation symmetry. The carbon content within DLN films is in the form of sp^2 and sp^3 phase. The G band is attributed to C-C bond stretching vibration of all pair of sp^2 hybridized carbon in both ring and chains of graphite layer for single crystalline graphite structure. While D band attributed well localized sp^2 bonded cluster as a breathing mode of hexagonal ring form graphitic structure within DLN network.[9,29–34] For any carbon based material, the sp^3 fraction is important parameter to investigate the mechanical properties of the films. The peak position and width of D and G bands and the intensity ratio of D and G peaks are well known characterization for hydrogenated and poor hydrogen free DLC based films.[35,36] Tamor and *et al.* suggested that, the increase of concentration of sp^3 carbon in the films induces the shift of the G band to the lower wavenumbers.[36] According to Richter and *et al.*, the shift of the G band due to the alteration of the force constant associated with variation of the sp^3 bonded fraction.[37] Again, Beeman *et al.* suggested that G band shifts in the lower frequency due to increase of sp^3 bonded atomic sites in amorphous carbon films.[38] The intensity and position of D and G peaks generally related with the ratio of sp^3:sp^2. This ratio can determine the mechanical and electrical

TABLE III. Gaussian analysis of Raman spectra of DLN films with different precursor flow rates by non-linear curve fitting method (where, ω: peak position, Γ: FWHM, I: integrated intensity).

Flow Rate (μl/min)	ω_D (cm^{-1})	Γ_D (cm^{-1})	ω_G (cm^{-1})	Γ_G (cm^{-1})	I_D/I_G
27.8	1377	238	1547	108	1.62
56.3	1379	268	1536	127	1.35
80.6	1365	181	1534	137	0.76
112.7	1390	263	1546	119	2.00
149.5	1400	259	1557	123	2.15

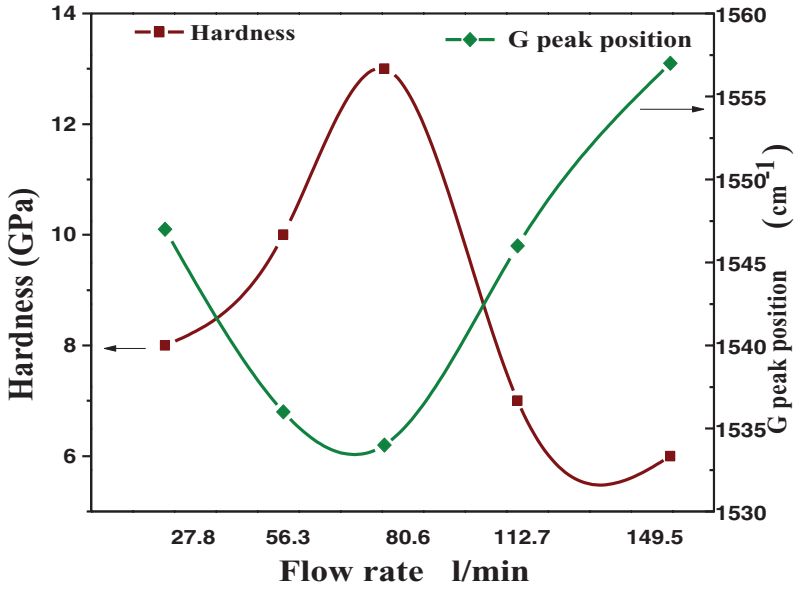

FIG. 5. Relationship between hardness and G peak position with different flow rate conditions DLN films.

properties of any diamond related films. The intensity ratio of D and G peaks (I_D/I_G) and full width half maxima (FWHM) are used as graphitization indices of the structure of carbon materials. Table III shows the peak position (ω), FWHM (Γ) and intensity ratio (I_D/I_G) in grater details of Gaussian deconvolution analysis of Raman spectroscopy. The I_D/I_G ratio can control the physical properties of the diamond films. As we know that the I_D/I_G ratio increases due to defect of graphitic lattice into the films, that means sp^2 phase will increase into the films which indicates the phase transformation of disordered diamond-like structure to ordered single crystal graphitic structure.[39–41] The intensity ratio decreases (1.62→0.76) continuously from 27.8 μl/min to 80.6 μl/min and its increases (0.76→2.15) continuously from 80.6 μl/min to 149.5 μl/min. The (I_D/I_G) becomes minimum (0.76) at 80.6 μl/min flow rate. At this flow rate the concentration of sp^3 content of the films is much higher compared to another flow rates. It means disorder diamond phase is much more during this flow rate compared to sp^2 based single crystalline graphitic layer. So at 80.6 μl/min flow rate, the hardness will be high (13GPa, see table V). For 149.5 μl/min, I_D/I_G ratio becomes higher (2.15) compare to any other flow rates which indicates the hardness is lower (6 GPa, see table V) in our experimental process. Fig. 5 shows the relationship between G peak position and hardness with different precursor flow rates of the DLN films. From this figure, it is clear that, when hardness of the films increases then shift of G peak decreases and when hardness decreases, then G peak shift increases.

The X-ray photoelectron spectroscopy (XPS) was applied for the investigation of the film surface composition of the DLN films. The experiment was performed for the binding energy from 0-1000 eV. Table IV shows the details about the concentration of different composition of DLN films with different precursor flow rates. From this table, the carbon content within the films decreases

TABLE IV. Percentage of film composition with different precursor flow rates as determined by XPS analysis.

Flow rate (μl/min)	% of C	% of Si	% of O	% of N
27.8	47.70	40.20	6.20	5.90
56.3	46.99	42.20	6.66	4.15
80.6	45.86	45.45	6.98	1.97
112.7	43.80	41.48	5.87	8.85
149.5	41.80	36.40	5.57	16.23

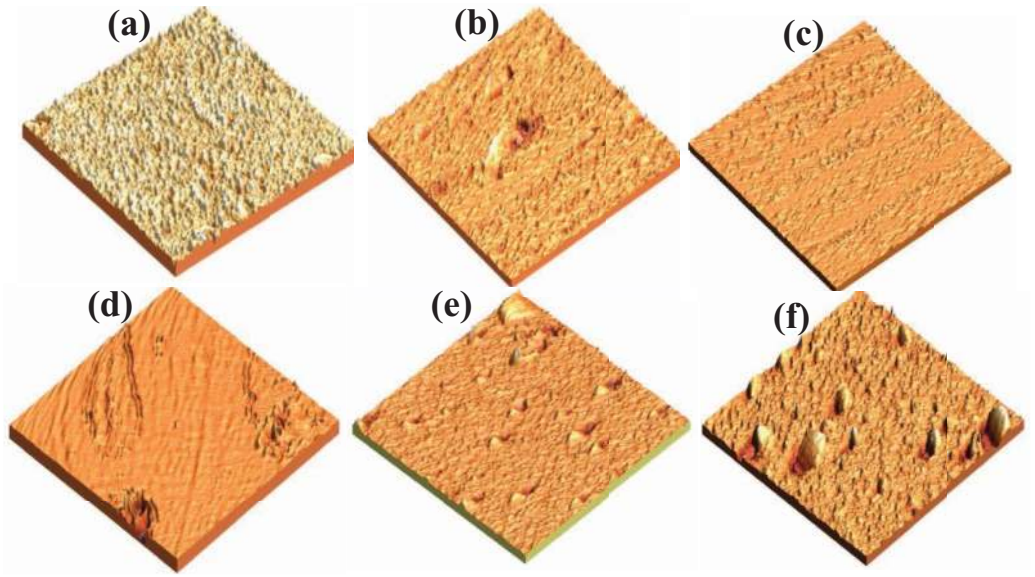

FIG. 6. AFM images of the DLN films (a) with out DLN coted pyrex glass slide. (b)-(f) DLN films with different flow rates (μl/min) (b) 27.8 (c) 56.3 (d) 80.6 (e) 112.7 (f) 149.5 [Scanning area for all image = 4 μm × 4 μm].

continuously with increase the flow rates from 27.8 μl/min to 80.6 μl/min. The concentration of silicon and oxygen increases continuously from the flow rate 27.8 μl/min to 80.6 μl/min and then decreases with increase the flow rate from 80.6 μl/min to149.5 μl/min. This increase of silicon content can improve the adhesion strength, reduce the internal stress of the films and improve the friction coefficient of the DLN films.[42,43] Silicon containing film may shows hydrophilic surface for the presence of silicon hydroxyl compounds with water molecules in environment. The nitrogen content of the DLN films decreases continuously from 27.8 μl/min to 80.6 μl/min and then increases rapidly from 80.6 μl/min to 149.5 μl/min flow rate. The increase of nitrogen content into the film can decrease the hardness,[22] but increase the silicon and oxygen content into the films can increase the hardness of the films.[44,45]

C. Tribological properties

The tribological properties of the DLN films were investigated by atomic force microscopy (AFM), nanoindentation test, and contact angle measurement technique. The surface morphologies of DLN films were analyzed by using atomic force microscope (AFM). Fig. 6 shows the three dimensional (3D) image of DLN films with different precursor flow rates. In this figure, sample (a) shows the surface morphology of clean pyrex glass substrate without DLN coated films where as samples (b)-(f) show the surface morphologies of DLN films with different precursor flow rates. Initially the surface roughness of DLN films is quite high (18.91 nm at flow rate 27.8 μl/min). But with increase of the flow rates, the surfaces become quite smooth from 27.8 μl/min to 80.6 μl/min

TABLE V. Tribological properties of DLN films with different flow rates.

Flow rate (μl/min)	Surface Roughness (nm)	Average roughness (nm)	Contact angle (deg)	Hardness (GPa)	Modulus of elasticity (GPa)
27.8	18.91	15.31	41.52	8	86
56.3	12.64	10.02	36.44	10	92
80.6	7.45	6.34	30.22	13	109
112.7	21.04	18.03	48.38	7	88
149.5	25.2	23.34	74.00	6	85

(see Figs. 6(b)–6(d)), after that the surface roughness again increases with increase of the flow rates from 80.6 μl/min to 149.5 μl/min (see Figs. 6(d)–6(f)). This increase of surface roughness might be due to the increase of silicon and oxygen content into the films (from the XPS study).[44,45] We have measured hardness, modulus of elasticity and contact angle of DLN films with different precursor flow rates. Table V shows the details about surface roughness, average roughness, hardness, modulus of elasticity and contact angle measurement with different precursor flow rates. As we compare Table IV and Table V, the hardness and modulus of elasticity are increased from 27.8 μl/min to 80.6 μl/min due to increase of silicon and oxygen content but decrease of nitrogen and carbon content into the films. Again from 80.6 μl/min to 149.5 μl/min the hardness and modulus of elasticity decreases due to increase of nitrogen and decrease of silicon and oxygen content into the films. The increase of silicon content (from27.8 μl/min to 80.6 μl/min) may increase the sp^3 fraction of the films by Raman spectroscopic analysis.[46] The maximum hardness and modulus of elasticity of the DLN films were 13 GPa and 109 GPa at flow rate 80.6 μl/min, where we found maximum silicon and oxygen content with less nitrogen content compare to any other flow rates. The surface contact angle is less (30.22°) at the flow rate 80.6 μl/min. This indicates that the film surface have more hydrophilic nature at flow rate 80.6 μl/min and after that contact angle increases continuously. The surface roughness decreases (7.45 nm) with decrease of contact angle (30.22°) and its increases (18.91 nm at flow rate 27.8 μl/min with contact angle 41.52° and 25.2 nm at flow rate 149.5 μl/min with contact angle 74°) with increase of contact angle (see table V).

IV. CONCLUSIONS

Diamond-like nanocomposite (DLN) thin films have been deposited on pyrex glass substrate using hexamethyldisiloxane (HMDSO) based liquid precursor by PECVD technique. The thickness and refractictive index of the films increase with the increase of the flow rates from 80.6μl/min to 112.7 μl/min and then they decrease slowly from 112.7 μl/min to 149.5 μl/min. The optical transparency of the films was maximum (94%) due to more oxygen and silicon content with less nitrogen content into the films at 80.6 μl/min. The transmission wavelength becomes larger (590-2000 nm) at 149.5 μl/min due to less carbon content within the films. FTIR spectroscopy shows that the DLN films have SiC_2, Si-C, Si-O, C-C, Si-H, C-H, N-H and O-H bonds with different peak position which decreases with increase of flow rate from 27.3-80.6 μl/min, and then increases again with increase the flow rates except N-H stretching. From Gaussian deconvolution method, the intensity ration (I_D/I_G) increases at 149.5μl/min due to increase of nitrogen and decrease of carbon contents into the films as a result, hardness and elastic modulus were decreased. From XPS composition analysis, we have found that the carbon content into the films decreases continuously but silicon and oxygen content increases continuously from 27.8 μl/min to 56.6 μl/min, and then decreases with increase of flow rate (149.5 μl/min). The increase of silicon content leads to increase of sp^3 fraction of carbon into the DLN films. As a result it helps to increase the hardness and modulus of elasticity of the films at 80.6μl/min. Also the increase of silicon at 80.6μl/min, can improve the adhesion properties and reduces the internal stress of the films. The results also show that much more oxygen content into the films improves the films quality (at 80.6 μl/min) but due to the increase of nitrogen content, film quality decreases sharply (at 149.5 μl/min). The surface roughness (7.45nm) and surface contact angle (30.22°) become minimum at 80.6 μl/min precursor

flow rate. The hardness and modulus of elasticity is 13 GPa and 109 GPa respectively at flow rate 80.6 μl/min. These values decrease if flow rate is decrease as well as increase from 80.6 μl/min. Finally, we conclude that the improved films quality can be achieved in the explained technique with the precursor flow rate between 56.3-112.7 μl/min, whereas in our study, 80.6 μl/min is the best precursor flow rate for the deposition of more advanced DLN films.

ACKNOWLEDGMENT

The authors (T. S. Santra and T. K. Barik) gratefully acknowledge the kind cooperation of Dr. Jagannath, BARC, Mumbai for his help in XPS measurement, and also Dr. A.S. Bhattacharyya NML, Jamshedpur for his cooperation in nanoindentation test. We would also like to express our heartfelt gratitude to Professor B. Mishra for Raman spectroscopic measurements respectively. We would also grateful to ESS-NTHU Micro-Nano Lab, Taiwan for AFM, UV-VIS spectroscopy and surface contact angle measurements.

[1] J. Robertson, Mater. Sci. Eng. R **37**, 129 (2002).
[2] Y. Lifshitz, Diamond Relat. Mater. **8**, 1659 (1999).
[3] W. Tillmann, E. Vogli, and F. Hoffmann, Thin Solid Films **516**, 262 (2007).
[4] D. Liu, G. Benstetter, and E. Lodermeier, Thin Solid Films **436**, 244 (2003).
[5] M. M. Morshed, B. P. McNamara, D. C. Cameron, and M. S. J. Hashmi, Surf. Coat. Techno. **163-164**, 541 (2003).
[6] B. Bushan, Diamond Relat. Mater. **8**, 1985 (1999).
[7] A. Shirakura, M. Nakaya, Y. Koga, H. Kodama, T. Hasebe, and T. Suzuki, Thin Solid Film **494**, 84 (2006).
[8] C. Venkatraman, D. J. Kester, A. Goel, and D. J. Bray, *International Conference on Surface Modification Technologies IX*, Cleveland, *The Minerals, Metals and Materials Society*, **21**, (1995).
[9] T. S. Santra, C. H. Liu, T. K. Bhatacharyya, P. Patel, and T. K. Barik, J. Appl. Phys. **107**, 124320 (2010).
[10] T. S. Santra, T. K. Bhatacharyya, P. Patel, F. G. Tseng, and T. K. Barik, Surf and Coat. Technol **206**, 228-233 (2011).
[11] T. S. Santra, T. K. Bhatacharyya, P. Mishra, F. G. Tseng, and T. K. Barik, Sci. Adv. Mater **4**,110-113 (2012).
[12] W. J. Yang, Y. H. Choa, T. Sekino, K. B. Shin, K. Niihara, and K. H. Auh, Mater. Lett. **57**, 3305 (2003).
[13] C. Ventakaraman, A. Goel, R. Lei, D. Kester, and C. Outten, Thin Solid Films **308-309**, 173 (1997).
[14] D. Neerinck, P. Persoone, M. Sercu, A. Goel, D. Kester, and D. Bray, Diamond Relat. Mater. **7**, 468 (1998).
[15] W. J. Yang, K. H. Auh, C. Li, and K. Niihara, J. Materials Sc. Letters **22**, 1261 (2003).
[16] B. Wei, B. Zhang, and K. E. Johnson, J. Appl. Phys. **83**, 2451 (1998).
[17] J. Hao, T. Xu, J. Zhang, and W. Liu, J. Phys. D: Appl. Phys. **39**, 1149 (2006).
[18] L. Y. Chen and F. C. N. Hong, Appl. Phys. Lett. **82**, 3526 (2003).
[19] V. Paishin, E. I. Meletis, S. Ves, and S. Logothetidis, Thin Solid Films **270**, 165 (1995).
[20] V. F. Dorfman and B. N. Pypkin, Surf. Coat. Techno. **48**, 193 (1991).
[21] V. F. Dorfman and B. N. Pypkin, U. S. Patent, Patent Number 5 352, 493 (1994).
[22] M. S. Hwang and C. Lee, Mater. Sci. Eng. B **75**, 24 (2000).
[23] D. A. Skoog, F. J. Holler, and T. A. Nieman, *Principles of Instrumental Analysis*, (4th ed., Harcourt Brace & Company, Philadelphia, 1998), Chap.16.
[24] M. P. Nadler, T. M. Donovan, and A. K. Green, Thin Solid Films **116**, 241 (1984).
[25] A. Ungureanu, O. D. Trong, E. Dumitriu, and S. Kaliaguine, Appl. Catalysis A **254**, 203 (2003).
[26] N. Mutsukura and K. Akita, Thin Solid Films **349**, 115 (1999).
[27] R. Heyner and G. Max, Thin Solid Films **258**, 14 (1995).
[28] T. Sharda, T. Soga, T. Jimbo, and M. Umeno, Appl. Phys. Lett. **80**, 2880 (2002).
[29] J. Wu, C. Chen, C. Shin, M. Li, M. Leu, and A. Li, Thin Solid Films **517**, 1141 (2008).
[30] S. Contarrini, E. Lambers, and P. H. Holloway, Appl. Surf. Sci. **62**, 181 (1992).
[31] W. J. Yang, Y. H. Choa, T. Sekino, K. B. Shim, K. Niihara, and K. H. Auh, Mater. Lett. **57**, 3305 (2003).
[32] R. Gago, M. Vinnichenko, H. U. Jager, A. U. Belov, I. Jimenez, N. Huang, H. Sun, and M. F. Maitz, Phys. Rev. B **72**, 014120 (2005).
[33] R. O. Dillion and J. A. Woollam, Phys. Rev. B **29**, 3482 (1984).
[34] S. Prawer and R. J. Nemanich, Phil.Trans. R. Soc. Lond. A **362**, 2537 (2004).
[35] M. Yoshikawa, Mater. Sci. Forum **365**, 52 (1998).
[36] M. A. Tomar and W. C. Vassell, J. Appl. phys **76**, 3823 (1994).
[37] A. Richter, H. J. Scheibe, W. Pompe, K. W. Brezeinka, and I. Muhling, J. Non-Cryst. Solids **88**, 131 (1986).
[38] D. Beeman, J. Silverman, R. Lynds, and M. R. Anderson, Phys. Rev. B **30**, 870 (1984).
[39] F. L. Feire, C. A. Achete, G. Mariotto, and R. Centeri, J. Vac. Sci. Technol. A **12**, 3048 (1994).
[40] W. J. Meng, and B. A. Gillispie, J. Appl. Phys. **84**, 4314 (1998).
[41] A. C. Ferrari and J. Robertson, Philo. Trans. Royl. Soc. A **362**(1824), 2477-2512 (2004).
[42] M. Ikeyama, S. Nakao, Y. Miyagawa, and S. Miyagawa, Surf. Coat. Techno. **191**, 38 (2005).
[43] S. G. Kim, S. W. Kim, N. Saitoand, and O. Takai, Diamond Relat. Mater. **19**, 1017 (2010).
[44] W. J. Wu, T. M. Pai, and M. H. Hon, Diamond Relat. Mater. **7**, 1478 (1998).
[45] P. Papakonstantinou, J. F. Zhao, P. Lemoine, E. T. McAsam, and J. A. McLaughlin, Diamond Relat. Mater. **11**, 1074 (2002).
[46] S. Ikeyama, S. Nkao, Y. Miyagawa, and S. Miyagawa, Surf. Coat. Techno. **191**, 38 (2005).